Plasma Radiation profiles measured with Imaging bolometers and their comparison with synthetic images from the impurity transport model for LHD

S.N.Pandya [1], B.J.Peterson [2], K. Mukai [2], M. Kobayashi [2], R. Sano [1] and E. Drapiko [3]

[1] *The Graduate University of Advanced Studies,322-6 Oroshi-cho, Toki, 509-5292, Japan*

[2] *National Institute for Fusion Science,322-6 Oroshi-cho, Toki, 509-5292, Japan*

[3] *Kurchatov Institute, Moscow 123182, Russia*

Introduction

The InfraRed imaging Video Bolometer (IRVB) [1] measures the radiation from the plasma in two dimensions (2D). The impurity radiation is also modeled by 3D edge impurity transport code EMC3-EIRENE [2,3]. A synthetic instrument has been developed which can trace the IRVB sight lines through the three dimensional impurity radiation results of the EMC3-EIRENE and generate a 2D image, which can be compared with the IRVB images quantitatively. This comparison is illustrated in this paper for studying the localization of the radiation near the X-point of the magnetic island used for sustaining plasma detachment. This work demonstrates the usefulness of the two dimensional images of the IRVBs in elucidating the three dimensional physics of a helical device.

IRVB concept

The IRVB has been developed in part to meet the challenging demands of the three dimensional (3D) physics of a helical device through the large number of channels and imaging capabilities afforded by this diagnostic. Currently four IRVBs are operational for studying 3D edge physics of LHD like the localization of radiation structures near the n/m=1/1 resonant magnetic perturbation (RMP) X-points during plasma detachment and also for 3D tomography on LHD. The IRVB is based on a thin 2.5μm platinum foil mounted in a frame inside a light shielding pipe. The side of the foil facing the plasma is collimated by an aperture and absorbs radiation from the plasma, which insures that each pixel of the IRVB has a unique line of sight. The other side of the foil is viewed by an infrared camera placed outside the LHD vacuum vessel in a double-walled soft-iron magnetic shield box, which is used to measure the 2D temperature distribution on the foil. The radiated power from the plasma falling on the foil can be estimated by numerically solving the 2D heat diffusion equation (1) using the spatiotemporal variation in the foil temperature obtained from the infrared camera.

$$S_{rad} = S_{bb} + C_s \frac{\partial T}{\partial t} - kt_f \left[\frac{\partial^2 T}{\partial x^2} + \frac{\partial^2 T}{\partial y^2} \right] \quad \text{Where} \quad S_{bb} = \varepsilon \sigma_{SB} (T^4 - T_0^4) \text{ is blackbody cooling term and } S_{rad} = \frac{P_{incident}}{l^2} \quad \ldots\ldots\ldots\ldots (1)$$

In this equation $P_{incident}$ is the power incident on the foil, T is the measured temperature, k, t_f and C_s are the thermal conductivity, thickness and surface thermal heat capacity of the foil respectively, l^2 is the area of IRVB pixel, σ_{SB} is the Stephen-Boltzmann constant and ε is the emissivity of the graphite coating used on the foil. Figure 1(a) illustrates the IRVB concept by a CAD layout and figure 1(b) shows the field of view (FoV) of the IRVB at the upper port of LHD. The IRVB images from the upper port are used in this work. The size of the IRVB foil is 100 X 130 mm^2 (poloidal X toroidal) subdivided into 18 X 24 IRVB pixels considering pinhole size of 8 X 8 mm^2. The noise equivalent power density of this IRVB is 20 $\mu W/cm^2$ which is estimated considering the camera sensitivity of 50 m°K, spatial and temporal averaging over the number of camera pixels and frames.

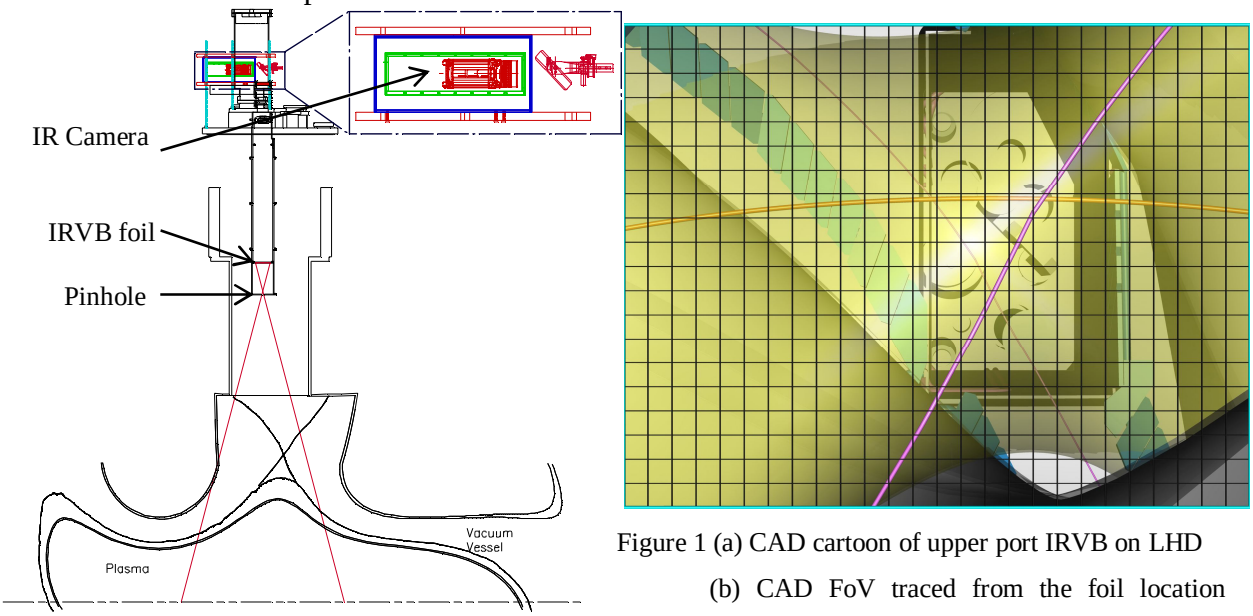

Figure 1 (a) CAD cartoon of upper port IRVB on LHD (b) CAD FoV traced from the foil location through the pinhole. The CAD shows IRVB pixels (grid), magnetic axis (yellow line), upper and lower helical divertor x-points (thick and thin pink lines respectively). FoV is flipped toroidally to compensate for mirror effect.

Plasma detachment and its stabilization in LHD

The power loads received by the diverter of a fusion device can be kept under acceptable limits by plasma detachment; hence it is prerequisite for future diverted magnetic confinement machines. Detachment in a tokamak is achieved by raising the plasma density to the density threshold but if the same is attempted with the LHD plasma, it terminates due to radiative collapse without detachment. Plasma detachment in LHD is attained and sustained by the addition of an n/m=1/1 resonant magnetic perturbation (RMP) [4] in the stochastic region with the help of 10 sets of saddle perturbation field coils. It is believed that the magnetic island helps to sustain the detachment by preventing the penetration of radiating zone into the core plasma, avoiding the radiative collapse. The EMC3-EIRENE 3D edge transport code predicts the radiation localization near the X-point of n/m=1/1 magnetic island during detachment as shown

by fig.2(b) whereas without RMP the radiation is found to be distributed uniformly throughout the stochastic edge shown by fig.2(a). A similar change in the radiative pattern is also observed experimentally by IRVBs installed at various strategic locations on LHD [5].

Synthetic Instrument

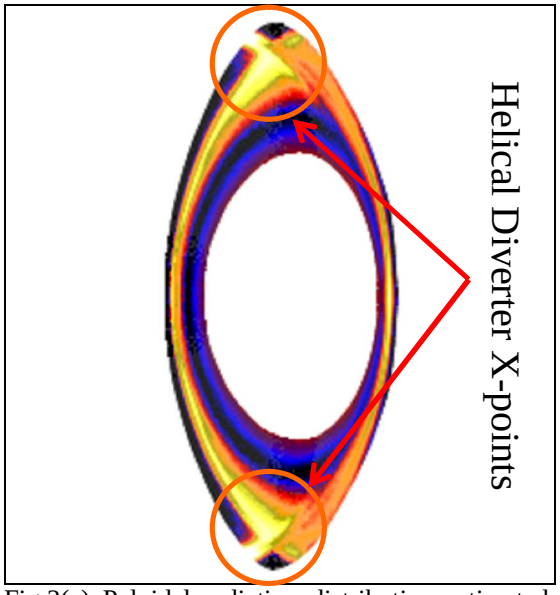

Fig.2(a) Poloidal radiation distribution estimated by EMC3-EIRENE with out RMP (attached)

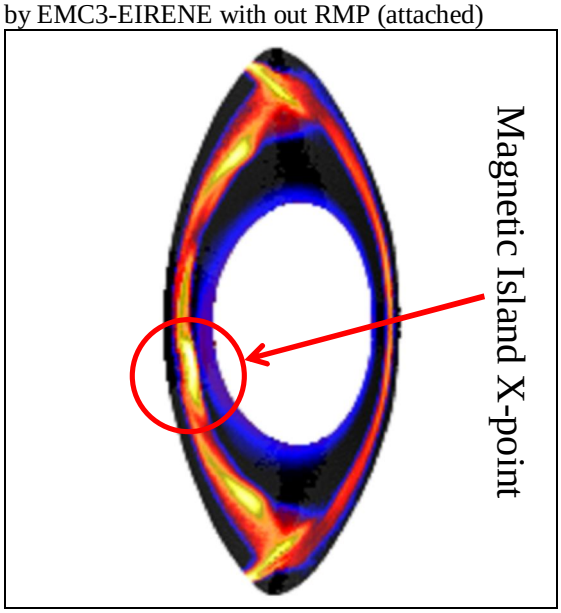

Fig.2(b) Poloidal radiation distribution estimated by EMC3-EIRENE with RMP (during detachment)

Since both modelling and experiments predicts the change in the radiation pattern it becomes crucial to study the degree of agreement between the results. A synthetic instrument consists of the geometry matrix, T_{ij}, which is generated by a code used to trace the sightlines for all the detectors of the IRVB through 3D radiation intensity distribution given by the EMC3-EIRENE and integrate the radiation for each sight line of the IRVB at the foil. This results in a 2D synthetic image of the plasma radiation at the IRVB foil which can easily be compared with the experimental data obtained from the IRVB experiments. The synthetic instrument estimates the power falling on IRVB detector by multiplying two matrices termed as emissivity matrix, S_j and geometry matrix, T_{ij}. S_j is obtained by regularizing and resampling the 3D radiation distribution obtained from EMC3-EIRENE into a course grid with radial and azimuth spatial resolution of 5 cm each and toroidal resolution of 1 º. T_{ij} is calculated by multiplying the detector solid angle Ω_{ij} (resulting from the IRVB pixel area and its distance from the sub-voxel) and the intersection volume $V_{ij,}$ (resulting from the intersection of the bolometer chord volume and the plasma volume). The power falling on the IRVB detector is given by equation (2).

$$P_i = \sum_j \frac{\Omega_{ij}}{4\pi} V_{ij} S_j = \sum_j T_{ij} S_j \quad \ldots\ldots(2)$$

A comparison between experiment and modeling is attempted in the next section for a discharge with RMP assisted detachment from the 16th LHD experimental campaign.

Modeling and Experiment – A comparison

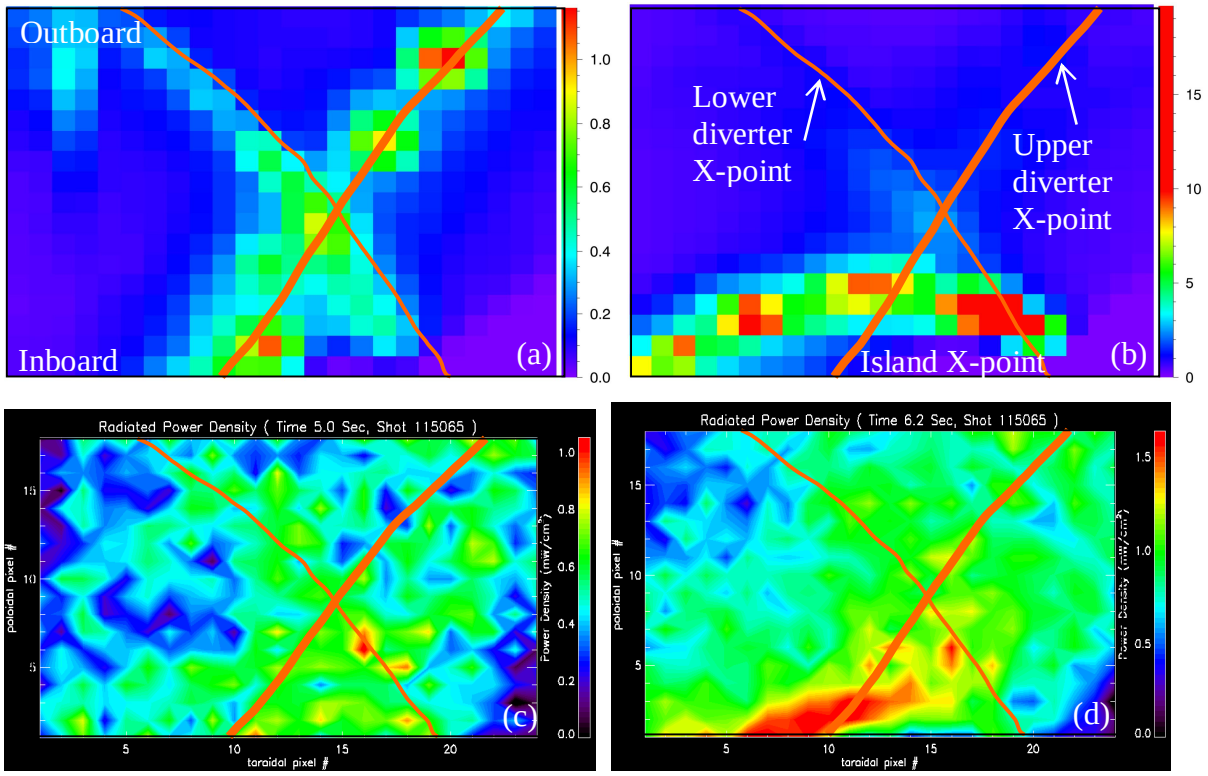

Fig. 3(a) and (b) Synthetic images with RMP for $\langle n_e \rangle = 4.0 \times 10^{-19}$ m^{-3} and 6.5×10^{-19} m^{-3} respectively

(c) and (d) Experimental IRVB images with RMP for $\langle n_e \rangle = 4.5 \times 10^{-19}$ m^{-3} and 8.0×10^{-19} m^{-3} respectively

Figure 3 establishes a comparison between the model and experimental images. Figure (a) and (c) shows a low density case when the plasma is still attached to the diverter. Modeling shows clear traces, both for upper and lower helical diverter X-points where as the experiment shows a strong trace along the upper X-point. The power densities for both the cases match very well. Figure (b) and (d) shows the high density case when the plasma is detached from the diverter. Both, modeling and experimental image shows clear localization of the radiation near the n/m=1/1 island X-point towards the inboard side of the torus. The power density from the model is 7 times higher than the experimentally observed value, the reason for which is still under investigation, but the resemblance in the change of radiation pattern for both cases is noteworthy.

Conclusion

This work illustrates the symbiotic relationship shared by 2D imaging diagnostics and 3D modeling techniques in unveiling the 3D physics for a complex device geometry like LHD.

Refrences

[1] B.J. Peterson, Rev. Sci. Instrum. **71,** 3696 (2000).
[2] Y. Feng et al., Contrib. Plasma Phys. **44**, 57 (2004).
[3] D. Reiter eta al., Fusion Sci. Technol. **47**, 172 (2005).
[4] M. Kobayashi *et al.* Phys. Plasmas **17,** 056111 (2010).
[5] B.J. Peterson *et al.* Journal of Nuclear Materials **415,** S1147 (2011).